

Least momentum space frustration as a condition for “high T_c sweet spot” in the iron-based superconductors

Hidetomo Usui¹, Katsuhiko Suzuki^{1,2}, and Kazuhiko Kuroki^{1,2}

¹Department of Engineering Science, The University of Electro-Communications, Chofu, Tokyo 182-8585, Japan

²JST, TRIP, Chiyoda, Tokyo 102-0075, Japan

E-mail: kuroki@vivace.e-one.uec.ac.jp

Abstract. In the present paper, we describe how the band structure and the Fermi surface of the iron-based superconductors vary as the Fe-As-Fe bond angle changes. We discuss how these Fermi surface configurations affect the superconductivity mediated by spin fluctuations, and show that in several situations, frustration in the sign of the gap function arises due to the repulsive pairing interactions that requires sign change of the order parameter. Such a frustration can result in nodes or very small gaps, and generally works destructively against superconductivity. Conversely, we propose that the optimal condition for superconductivity is realized for the Fermi surface configuration that gives the least frustration while maximizing the Fermi surface multiplicity. This is realized when there are three hole Fermi surfaces, where two of them have $d_{XZ/YZ}$ orbital character and one has $d_{X^2-Y^2}$ for all k_z in the three dimensional Brillouin zone. Looking at the band structures of various iron-based superconductors, the occurrence of such a “sweet spot” situation is limited to a narrow window.

1. Introduction

The discovery of high temperature superconductivity in the iron-based superconductors[1] has attracted much attention in many aspects. Not only the high T_c itself, but also a number of experiments indicating non-universality of the superconducting gap function, such as sign reversing, anisotropy, or the presence of nodes, suggest an unconventional pairing mechanism. Most probable candidate for such an unconventional mechanism is the pairing mediated by spin fluctuations, where the superconducting gap changes sign between the disconnected Fermi surfaces, namely, the so-called $s\pm$ pairing[2, 3].

Back in 2001, one of the present authors proposed that spin fluctuation mediated pairing in systems with nested disconnected Fermi surfaces may give rise to a very high T_c superconductivity[4, 5]. The idea is that the repulsive pairing interaction mediated by spin fluctuations can be fully exploited without introducing nodes of the superconducting gap on the Fermi surfaces. Although the Fermi surface of the iron-based superconductors does resemble the proposed Fermi surface configuration, there are some important differences. One is that the Fermi surface in the iron-based superconductors has multiple orbital characters, and second is that there can be frustrations in the sign of the gap function, which can give rise to gap nodes on the Fermi surface. In the present paper, we focus on this gap-sign frustration problem, and propose that the Fermi surface configuration that gives the least frustration provides the optimal condition for high T_c in the iron-based superconductors. In ref.[6], two of the present authors pointed out that maximizing the Fermi surface multiplicity leads to the optimization for T_c , but considering the frustration problem studied in the present paper, the “sweet spot” for high T_c is further limited to a narrow window of the Fermi surface configuration.

2. Typical band structure and Fermi surfaces

Let us first describe the band structure of LaFeAsO. LaFeAsO takes a layered structure, where Fe atoms form a square lattice in each layer, sandwiched by As atoms with tetrahedral coordination. We use the band structure obtained from first principles[7] to construct the maximally localized Wannier functions[8]. These Wannier functions have five orbital symmetries ($d_{3Z^2-R^2}$, d_{XZ} , d_{YZ} , $d_{X^2-Y^2}$, d_{XY}), where X, Y, Z refer to those for this unit cell with two Fe sites as shown in Fig.1(a). The two Wannier orbitals in each unit cell are equivalent in that each Fe atom has the same local arrangement of other atoms. We can then take a unit cell that contains only one orbital per symmetry by unfolding the Brillouin zone, and an effective five-band model on a square lattice is obtained, where x and y axes are rotated by 45 degrees from X - Y .

In Fig.1(b) (right), the Fermi surface for 10 percent electron doping is shown in the two-dimensional unfolded Brillouin zone. The Fermi surface consists of four pieces: two concentric hole pockets (denoted here as α_1 , α_2) centered around $(k_x, k_y) = (0, 0)$, two electron pockets around $(\pi, 0)$ (β_1) or $(0, \pi)$ (β_2), respectively. Besides these pieces of the Fermi surface, there is a portion of the band near (π, π) that touches the E_F , so that the

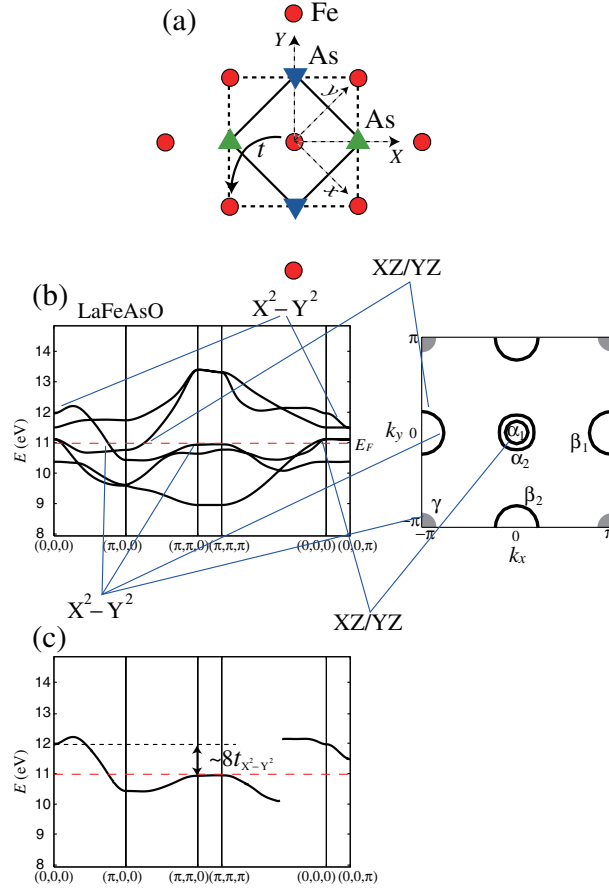


Figure 1. (a) The original (dashed lines) and reduced (solid) unit cells with \bullet (Fe), ∇ (As below the Fe plane) and \triangle (above Fe). (b) The band structure (left) of the five-band model for LaFeAsO, and the Fermi surface (right) at $k_z = 0$ for 10 percent electron doping. The main orbital characters of some portions of the bands and the Fermi surface are indicated. The dashed horizontal line in the band structure indicates the Fermi level for 10 percent electron doping. The short arrow in the band structure indicates the position of the Dirac cone closest to the Fermi level. The gray areas in the Fermi surface around the zone corners represent the γ Fermi surface, which is barely absent for 10 percent electron doping. (c) The portion of the band that has mainly the $d_{X^2-Y^2}$ orbital character.

portion acts as a “quasi Fermi surface (γ)” around (π, π) . As for the orbital character, α and portions of β near Brillouin zone edge have mainly d_{XZ} and d_{YZ} character, while the portions of β away from the Brillouin zone edge and γ have mainly $d_{X^2-Y^2}$ orbital character (see also Fig.1(c)).

3. Fermi surface appearance/disappearance against the bond angle

The band structure and the Fermi surfaces of the iron-based superconductors are sensitive to the lattice structure. In this section, we consider hypothetical lattice

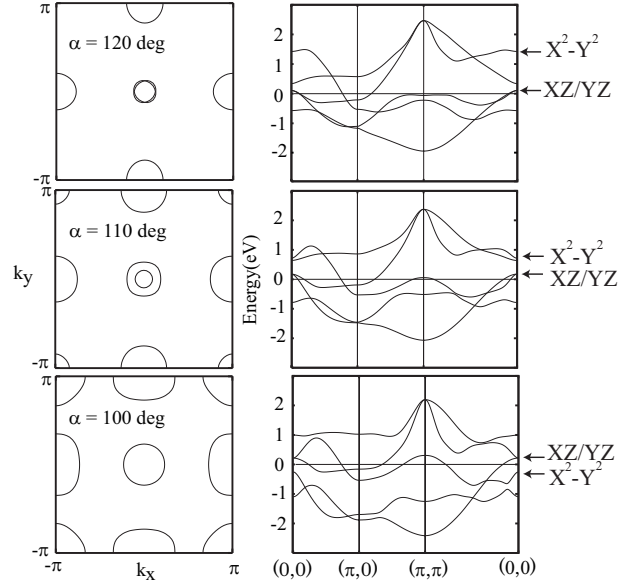


Figure 2. The band structure and the Fermi surface of hypothetical lattice structures of LaFeAsO with varying the Fe-As-Fe bond angle while fixing the Fe-As bond length to its original value. Position of the bands having $X^2 - Y^2$ and XZ/YZ orbital characters at $(0,0)$ is indicated.

structures of LaFeAsO, where we fix the bond length at its original length and vary the bond angle α (Fig.2(a))[6]. We first neglect the three dimensionality (out-of-plane hoppings), and consider a two dimensional model. The Fermi surface is obtained for 10 percent electron doping. When the bond angle is large, two hole Fermi surfaces, α_1 and α_2 are present around the wave vector $(0,0)$, while the γ around (π, π) is missing. As α decreases, the γ Fermi surface appears around (π, π) , and there are now three hole Fermi surfaces. This appearance of the additional Fermi surface has been noticed as an effect of increasing the pnictogen height [9, 10, 16, 11, 12]. When α is further reduced, the α_1 Fermi surface disappears, and again the Fermi surface multiplicity reduces to two, but in this case one around $(0, 0)$ and another around (π, π) . Such a disappearance of the α_1 hole Fermi surface was first noticed in the band calculation of $\text{Ca}_2\text{Al}_4\text{O}_6\text{Fe}_2\text{As}_2$ [13] by Miyake *et al.* in refs.[14, 15]. This material indeed has very small bond angle of about 102 degrees.

Fig.3 explains schematically the band structure/Fermi surface variation against the bond angle reduction[14]. As the bond angle is reduced, the $X^2 - Y^2$ band below the Fermi level around (π, π) rises up, while another $X^2 - Y^2$ portion of the band above the Fermi level around $(0, 0)$ comes down. This band deformation can be understood from Fig.1(c), where the $X^2 - Y^2$ portion of the band for the original LaFeAsO is extracted. In the tightbinding picture, the energy difference between the wave vectors $(0, 0)$ and (π, π) is roughly equal to $8t_{X^2-Y^2}$, where $t_{X^2-Y^2}$ is the nearest neighbor hopping of the $X^2 - Y^2$ orbital. As the bond angle is reduced, the contribution to $t_{X^2-Y^2}$ from the $\text{Fe} \rightarrow \text{As} \rightarrow \text{Fe}$ path decreases, while that from the direct $\text{Fe} \rightarrow \text{Fe}$ path increases. The two

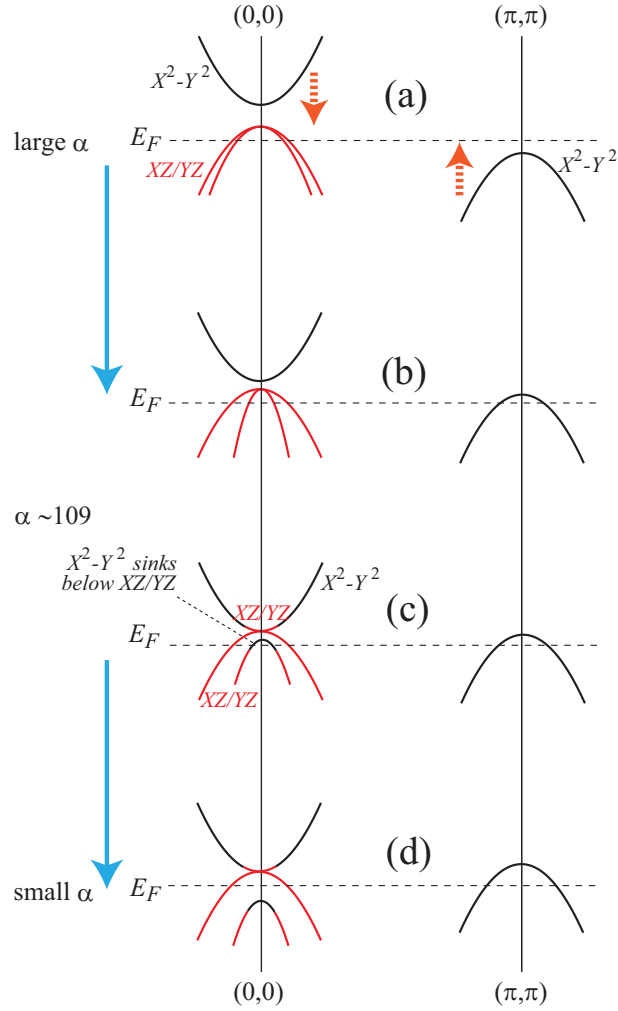


Figure 3. A schematic figure for the band structure variation against the bond angle α . The black (red) portions indicate the bands with strong $X^2 - Y^2$ (XZ/YZ) orbital character.

contributions have opposite signs, so that the reduction of the bond angle results in a decrease of $t_{X^2-Y^2}$ [14].

When the bottom of the upper $X^2 - Y^2$ portion sinks below the XZ/YZ bands around $(0, 0)$, a band structure reconstruction takes place, and now the two bands that are degenerate at $(0, 0)$ repel with each other (one going up, the other going down) as the wave vector moves away from $(0, 0)$ (Fig.3(c)). In this situation, the band below these two bands has $X^2 - Y^2$ character near $(0, 0)$, and changes its character to XZ/YZ as the wave number increases. Therefore, just before the inner hole (α_1) Fermi surface disappears, it has strong $X^2 - Y^2$ character.

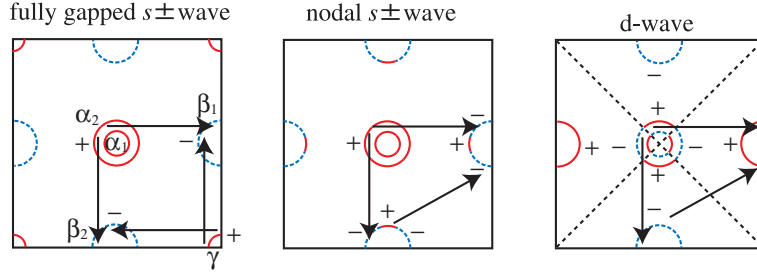


Figure 4. The fully-gapped $s\pm$ wave, the nodal $s\pm$ wave and d wave gap are schematically shown. The solid red (dashed blue) curves represent positive (negative) sign of the gap. The arrows indicate the dominating nesting vectors.

4. Frustration in the superconducting gap in the absence of γ Fermi surface : a brief review

Having understood the Fermi surface variation against the bond angle, we now consider how this should affect the gap function of the superconductivity mediated by spin fluctuations. The pairing interaction mediated by spin fluctuations is repulsive, so the superconducting gap has a tendency of changing its sign between the initial and final wave vectors of the pair scattering. Another important point is that the spin fluctuations develop at wave vectors that bridge the portions of the Fermi surface having the same orbital character[16].

In the presence of the $X^2 - Y^2$ originated γ and XZ/YZ originated α_1 and α_2 Fermi surfaces (case (b) in Fig.3), it is known that the γ - β interaction among portions having $X^2 - Y^2$ character and the α - β interactions among portions with XZ/YZ character dominate, and the superconducting gap is fully open on all the Fermi surfaces while changing its sign as $+$, $-$, $+$ along α , β , γ Fermi surfaces. This is the fully gapped $s\pm$ gap[16, 17, 18].

On the other hand, in the absence of the γ Fermi surface (case (a) in Fig.3), the pairing interaction between the $X^2 - Y^2$ portions of the β Fermi surfaces and that between the XZ/YZ portions of the α and β Fermi surfaces results in a frustration in the sign of the gap function. This situation was studied in several previous papers[19, 16, 17, 18]. This can result in either nodal $s\pm$ -wave or d -wave pairings, where the nodes of the gap go into the β Fermi surface in the former, and α in the latter. A schematic figure summarizing the above is shown in Fig.4[16]. As was shown in ref.[16], this frustration effect degrades T_c of the superconductivity, so that the lattice structure acts as a switch between high T_c nodeless and low T_c nodal superconductivity.

5. Frustration in the case of nearly vanishing α_1 Fermi surface

Here we discuss another situation where the frustration arises in the sign of the superconducting gap function. As mentioned in section 3, the $X^2 - Y^2$ orbital character strongly mixes into the α_1 Fermi surface just before the Fermi surface vanishes as the

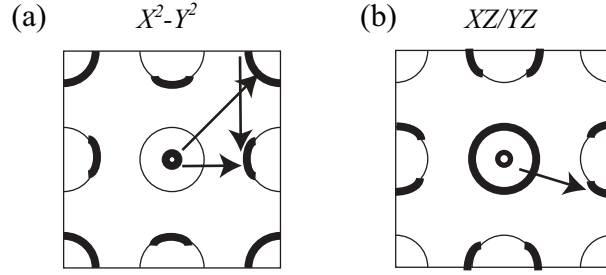


Figure 5. Dominating pairing interactions for the (a) $X^2 - Y^2$ and (b) XZ/YZ portions of the Fermi surface in the case where the inner hole Fermi surface (α_1) is barely present. In this case, α_1 is a mixture of $X^2 - Y^2$ and XZ/YZ .

bond angle is reduced. In this situation, there are now $X^2 - Y^2$ components on α_1 , β , and γ (if present) Fermi surfaces. Since these Fermi surfaces interact with repulsive pairing interactions, once again, a frustration arises in the sign of the superconducting gap (Fig.5(a)). In addition to this, there can also be some XZ/YZ component remaining in the α_1 Fermi surface, and this portion tends to change the sign from the β Fermi surfaces (Fig.5(b)) so this can be another factor for the frustration.

To actually see this frustration effect, here we consider hypothetical lattice structures of $\text{Ca}_4\text{Al}_2\text{O}_6\text{Fe}_2\text{As}_2$ [13], where we vary the bond angle from 108 to 109 degrees, and contrast a two dimensional five orbital model in the unfolded Brillouin zone. In this angle regime, the α_1 Fermi surface is barely present, and it is indeed composed of mixed $X^2 - Y^2$ and XZ/YZ orbital components. We apply fluctuation exchange approximation to this model[20], and obtain the eigenfunction (gap function) of the linearized Eliashberg equation as was done in ref.[6]. In Fig.6, we show the gap function for the two angles for 10 percent electron doping and temperature $T = 0.01\text{eV}$. It can be seen that the magnitude of the gap on the α_1 Fermi surface is very small, and its sign actually changes as the bond angle is varied, reflecting the frustration.

6. Effect of three dimensionality

When the systems exhibit some three dimensionality, the above mentioned variation of the Fermi surface configuration against the bond angle depends on k_z . This is shown schematically in Fig.7. In systems with moderate three dimensionality, the orbital character change of the α_1 Fermi surface and its disappearance first starts at $k_z = \pi$ (around Z point) as the bond angle is reduced, and ends at $k_z = 0$ (Γ point). Namely, the α_1 Fermi surface becomes three dimensional before it disappears completely. In this case, the above mentioned frustration effect should be present around the top and the bottom portions of the three dimensional Fermi surface.

In fact, the above mentioned three dimensionality of the band structure is rather common for the iron-based superconductors. This has been discussed in detail in ref.[12]. In Fig.8, we show the band structure of various iron-based superconductors for $k_z = 0$

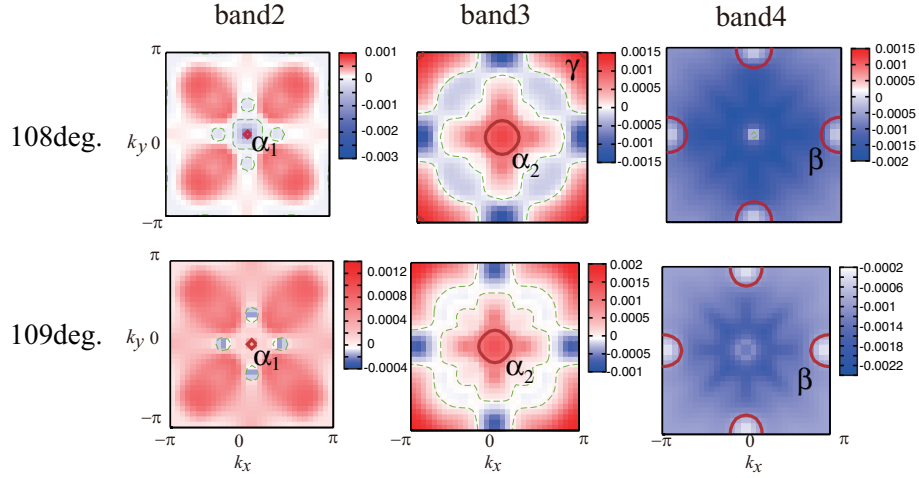


Figure 6. The gap function obtained by FLEX for the hypothetical lattice structures of $\text{Ca}_4\text{Al}_2\text{O}_6\text{Fe}_2\text{As}_2$. The bond angle α is varied to 108 or 109 degrees, while the bond length is fixed to the original value.

and $k_z = \pi$ planes (in the original folded Brillouin zone) calculated by using the Wien2k package[21]. One can see that, except for LaFeAsO , the two bands degenerate at Z point $(0, 0, \pi)$ repel with each other as the wave vector moves away from Z in the $k_z = \pi$ plane. This means that configurations (c) or (d) in Fig.3 are realized for a certain range of k_z . On the other hand, in FeSe , LiFeAs and BaFe_2As_2 the band structure near the $k_z = 0$ plane takes configuration (b), so that in these materials, the band structure near the Fermi level is indeed three dimensional.

Conversely, the 1111 systems can be considered as somewhat exceptional in that, although the three dimensional $X^2 - Y^2$ band does exist, it does not come down too rapidly before the $X^2 - Y^2$ originated γ Fermi surface appears. In fact, NdFeAsO , one of the materials having the highest T_c , seems to have the least frustration from the above mentioned viewpoint. Namely, as seen in the band structure shown in Fig.9 in the unfolded Brillouin zone[16], the γ Fermi surface is present but the three dimensional $X^2 - Y^2$ band still lies above the XZ/YZ bands for all k_z . On the other hand, from the comparison to the band structure of LaFeAsO (Fig.1(b)), it can be seen that as a trade-off for the appearance of the γ Fermi surface around (π, π) , the three dimensional $X^2 - Y^2$ band along $(0, 0, 0)$ - $(0, 0, \pi)$ has certainly come down very close to the XZ/YZ band, and for smaller bond angle or higher pnictogen position, the band reconstruction and thus the frustration starts to take place. Therefore, from the present viewpoint, the “sweet spot” for high T_c is restricted to a narrow window, which may explain the experimental observations[22, 23].

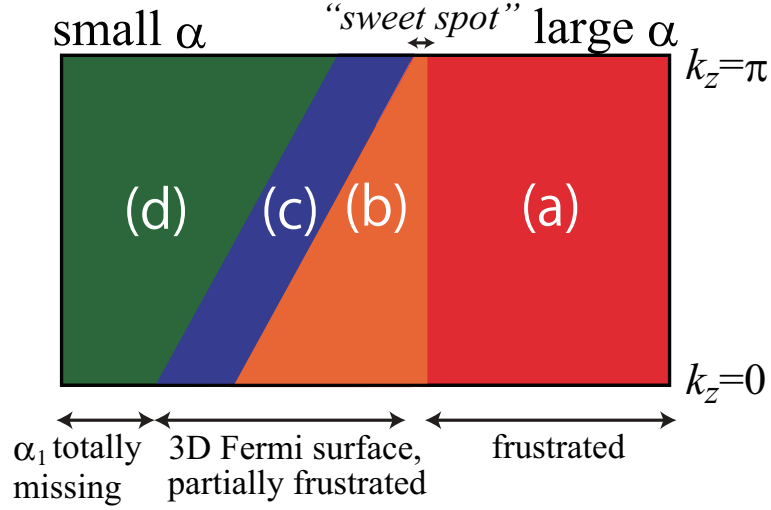


Figure 7. A schematic figure representing the band structure and the hole Fermi surface variation against the bond angle for moderately three dimensional systems. (a) to (d) correspond to the configurations shown in Fig.3. The “sweet spot” is restricted to the regime where the $X^2 - Y^2$ originated γ Fermi surface is effective and the α_1 Fermi surface has XZ/YZ character for all k_z .

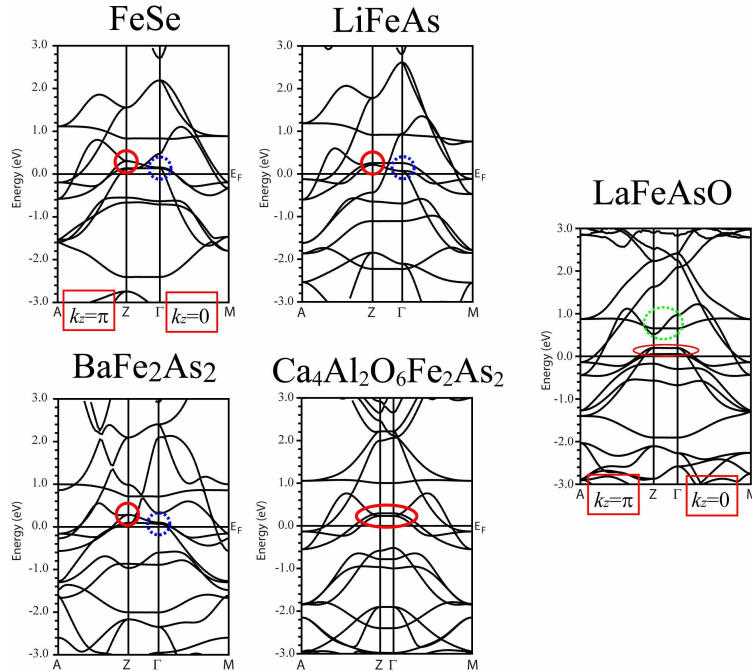


Figure 8. First principles band structure for various iron-based superconductors. $k_z = 0$ and $k_z = \pi$ planes are shown. The red solid circles (or ellipse) indicates the portion where the two bands degenerate at wave vector $(k_x, k_y) = (0, 0)$ repel with each other as the wave number increases, while the dashed blue circles are the portions where the two bands degenerate at $(0, 0)$ both form a hole Fermi surface. For LaFeAsO, a typical example for 1111 systems, the three dimensional band along Γ -Z having $X^2 - Y^2$ character (green dashed ellipse) stays above the degenerate XZ/YZ bands (red solid).

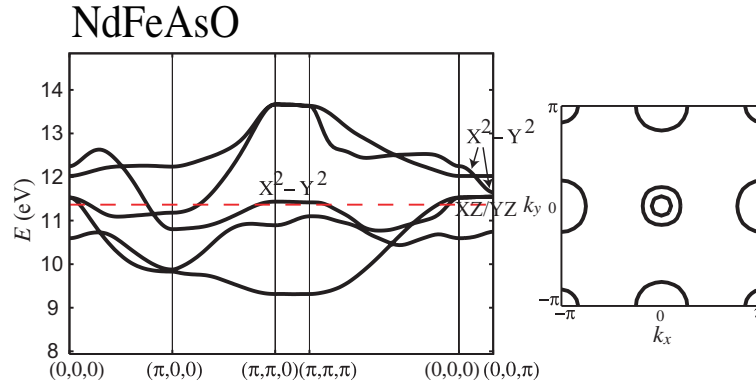


Figure 9. The band structure of NdFeAsO in the unfolded Brillouin zone. The Fermi level is for 10 percent electron doping. The two conditions for least frustration is satisfied: (i) the $X^2 - Y^2$ Fermi surface is present around the wave vector (π, π) , and (ii) the three dimensional $X^2 - Y^2$ band from $(0, 0, 0)$ to $(0, 0, \pi)$ does not intersect the XZ/YZ bands for all k_z .

7. Conclusion

As described in the present paper, the multiplicity of the Fermi surfaces and even their orbital characters change as the lattice structure is varied. Because of the presence of multiple Fermi surfaces and the repulsive pairing interaction mediated by the spin fluctuations, frustration can arise in the sign of the gap on the disconnected Fermi surfaces. This can result in nodal structures in the gap function, and should generally work destructively against superconductivity. Conversely, from the present viewpoint, the optimal situation for the spin fluctuation mediated superconductivity is when the $X^2 - Y^2$ γ Fermi surface is effective and the α_1 Fermi surface has XZ/YZ orbital character for *all* k_z . As far as the first principles band calculations are concerned, this situation is realized in limited materials like NdFeAsO and SmFeAsO, where the highest T_c among the iron based superconductors is observed experimentally. From this viewpoint, further band structure calculation studies may give useful information for obtaining new related superconductors with higher T_c .

Acknowledgment

We acknowledge C.H. Lee, T. Miyake, O.K. Andersen, H. Mukuda, H. Kinouchi, and Y. Kitaoka for illuminating discussions.

References

- [1] Y.Kamihara, T.Watanabe, M.Hirano, and H. Hosono, J. Am. Chem. Soc. **130**, 3296 (2008).
- [2] I.I. Mazin, D.J. Singh, M.D. Johannes, and M.H. Du, Phys. Rev. Lett. **101**, 057003 (2008).
- [3] K.Kuroki, S.Onari, R.Arita, H.Usui, Y.Tanaka, H.Kontani, and H.Aoki, Phys. Rev. Lett. **101**, 087004 (2008).

- [4] K. Kuroki and R. Arita, Phys. Rev. B **64**, 024501 (2001).
- [5] K. Kuroki, T. Kimura and R. Arita, Phys. Rev. B **66**, 184508 (2002).
- [6] H. Usui and K. Kuroki, Phys. Rev. B **84**, 024505 (2011).
- [7] S. Baroni, A. Dal Corso, S. de Gironcoli, P. Giannozzi, C. Cavazzoni, G. Ballabio, S. Scandolo, G. Chiarotti, P. Focher, A. Pasquarello, K. Laasonen, A. Trave, R. Car, N. Marzari and A. Kokalj, <http://www.quantum-espresso.org/>.
- [8] N. Marzari and D. Vanderbilt, Phys. Rev. B **56**, 12847 (1997); I. Souza, N. Marzari and D. Vanderbilt, Phys. Rev. B **65**, 035109 (2001). The Wannier functions are generated by the code developed by A. A. Mostofi, J. R. Yates, N. Marzari, I. Souza and D. Vanderbilt, (<http://www.wannier.org/>).
- [9] D.J.Singh and M.H. Du, Phys. Rev. Lett. **100**, 237003 (2008).
- [10] V. Vildosola, L. Pourovskii, R. Arita, S. Biermann, and A. Georges, Phys. Rev. B **78**, 064518 (2008).
- [11] S. Lebegue, Z.P. Yin, and W.E. Pickett, New J. Phys. **11**, 025004 (2009).
- [12] O.K. Andersen and L. Boeri, Annalen der Physik, **1** 8 (2011).
- [13] P.M. Shirage, K. Kihou, C.H. Lee, H. Kito, H. Eisaki, and A. Iyo, Applied Physics Letters **97** 172506 (2010).
- [14] T. Miyake, T. Kosugi, S. Ishibashi, and K. Terakura, J. Phys. Soc. Jpn. **79**, 123713 (2010).
- [15] T. Kosugi, T. Miyake, S. Ishibashi, and K. Terakura, J. Phys. Soc. Jpn. **81**, 014701 (2012).
- [16] K. Kuroki, H. Usui, S. Onari, R. Arita, and H. Aoki, Phys. Rev. B **79**, 224511 (2009).
- [17] F. Wang, H. Zhai, and D.-H. Lee, Phys. Rev. B **81**, 184512 (2010).
- [18] R. Thomale, C. Platt, W. Hanke, and B.A. Bernevig, Phys. Rev. Lett. **106**, 187003 (2011).
- [19] S. Graser, T. A. Maier, P. J. Hirschfeld, and D. J. Scalapino, New J. Phys. **11**, 025016 (2009).
- [20] N.E. Bickers, D.J. Scalapino, and S.R. White, Phys. Rev. Lett. **62**, 961 (1989).
- [21] P. Blaha, K. Schwarz, G. K. H. Madsen, D. Kvasnicka, J. Luitz In WIEN2K, An Augmented Plane Wave + Local Orbitals Program for Calculating Crystal Properties, (Karlheinz Schwarz/ Techn. Universität Wien, Wien, Austria, 2001).
- [22] C.H. Lee, A.Iyo, H. Eisaki, H. Kito, M.T. Fernandez-Diaz, T. Ito, K. Kihou, H. Matsuhata, M. Braden, and K. Yamada, J. Phys. Soc. Jpn. **77**, 083704 (2008).
- [23] Y. Mizuguchi and Y. Takano, J. Phys. Soc. Jpn. **79**, 102001 (2010) and references therein.